



# Bayesian Conditional Autoregressive for Rainfall Modeling in East Java

Suci Astutik\*, Evellin Dewi Lusiana, Nur Kamilah Sa'diyah, Rismania Hartanti Putri Yulianing Damayanti, Fidia Raaihatul Mashfia, Agus Yarcana, Fang You Dwi Ayu Shalu Saniyawati, Ulfah Fauziyyah Hidayat, Aurora Gema Bulan Octavia

*Department of Statistics, Faculty of Mathematics and Sciences, Universitas Brawijaya, Indonesia*

**Abstract** Rainfall in East Java has high spatial variation, requiring a modeling approach that can capture inter-regional dependencies. This study aims to estimate rainfall patterns using Bayesian Conditional Autoregressive (BCAR) models that incorporate spatial effects, specifically the Intrinsic Conditional Autoregressive (ICAR) and Leroux CAR specifications. Parameter estimation was conducted using Markov Chain Monte Carlo (MCMC) methods to ensure convergence and posterior stability. Monthly rainfall data from East Java during the 2022–2023 were analyzed by dividing the period into the transition to the rainy season (September–November) and the rainy season (December–February). The results indicate that during the rainy season, most climatic variables, including temperature, humidity, wind direction, and cloud cover, do not show statistically significant effects on rainfall, whereas during the transition season, wind exhibits a significant positive influence. Comparative model evaluation reveals that the ICAR model provides the best predictive performance, as indicated by the lowest Root Mean Square Error (RMSE), while the Leroux CAR model demonstrates consistent estimation of spatial dependence across both periods. Simulation results further confirm that the parameter estimators are unbiased, as evidenced by the close agreement between simulated parameters and empirical data estimates. These findings demonstrate that BCAR models, particularly the ICAR specification, are effective in capturing spatial rainfall variability in East Java. This study contributes methodologically to spatial climatological analysis and provides a foundation for future research incorporating additional covariates and extended temporal coverage to enhance rainfall prediction accuracy.

**Keywords** Bayesian, Conditional Autoregressive Model, Rainfall, Spatial.

**AMS 2010 subject classifications:** 62C10, 62F15

**DOI:** 10.19139/soic-2310-5070-3030

## 1. Introduction

*Statistical* approaches have long played an important role in modeling complex environmental phenomena, including rainfall. Classical regression and spatial models like SAR and SEM, while widely used, often face limitations due to restrictive assumptions, hindering their effectiveness when dealing with high spatial heterogeneity and uncertainty. Maximum Likelihood Estimation (MLE) becomes less efficient when the assumptions of normality and homoscedasticity are violated [1, 2]. To overcome these limitations, the Bayesian paradigm offers a flexible alternative by allowing the incorporation of prior knowledge and generating posterior distributions that quantify uncertainty more comprehensively[5].

One of the important developments within the Bayesian framework is the CAR model. This approach is particularly suited for spatially referenced data defined over administrative areas, where neighborhood structures can be explicitly modeled through adjacency matrices [3]. Unlike point-based geostatistical models, the CAR model effectively captures local variations and spatial dependence at the areal level [3]. The Bayesian CAR model

---

\*Correspondence to: Suci Astutik (Email: suci\_sp@ub.ac.id). Department of Statistics, Universitas Brawijaya, Veteran Road, Malang, Indonesia (65145).

also enables inference through simulation-based techniques such as MCMC, which provide not only parameter estimates but also predictive distributions useful for long-term projections [6]. The advantage of this approach lies in its ability to flexibly accommodate spatial dependence, manage data limitations through prior information, and produce credible intervals that enrich interpretation beyond point estimates.

In the context of hydrometeorology, rainfall is one of the most critical variables influenced by climate dynamics [7]. Numerous studies have modeled rainfall with a variety of statistical and machine learning techniques. For example, applied a Bayesian state-space approach for spatio-temporal rainfall [8], Geographically Weighted Regression (GWR) [9], used GSTAR models for East Java rainfall data [11]. Other studies employed Bayesian Hidden Markov Models [12, 10] and artificial neural networks [13, 14, 15]. Despite these advances, the application of Bayesian CAR models in rainfall modeling—particularly in Indonesia—remains limited, even though such models hold promise for capturing areal-level spatial dependencies inherent in climatic and hydrometeorological processes.

Indonesia, as an archipelagic country located in the tropics, is highly vulnerable to hydrometeorological disasters such as floods, droughts, and landslides [16]. Rainfall variability, strongly affected by climate change and phenomena such as El Niño and La Niña, plays a central role in shaping these risks. The La Niña phenomenon, in particular, is associated with increased rainfall intensity and heightened flood risk across many regions, including East Java [17, 18]. Accurate spatial modeling of rainfall during such events is therefore crucial for disaster risk reduction, climate adaptation planning, and water resource management.

This study aims to apply and compare BCAR models for analyzing spatial rainfall patterns in East Java, Indonesia, during the La Niña period. Specifically, this study models and maps the spatial distribution of rainfall using two BCAR specifications, namely the ICAR and Leroux CAR models, which explicitly account for spatial dependence across districts and municipalities. As a benchmark, a conventional non-spatial linear regression model is also considered to illustrate the limitations of ignoring spatial autocorrelation in rainfall data. This study evaluates and compares the performance of the non-spatial and spatial models through posterior summaries, credible intervals, and predictive accuracy measures, particularly the RMSE complemented by spatial prediction maps. The comparative analysis is intended to demonstrate that models incorporating spatial structure provide more accurate and reliable rainfall predictions than non-spatial approaches.

The findings are expected to contribute both methodologically and practically. From a methodological perspective, this study extends the application of Bayesian CAR models for hydrometeorological data in the Indonesian context by providing a systematic comparison between ICAR, Leroux CAR, and non-spatial linear regression models. From a practical perspective, the results may serve as a scientific basis for relevant agencies in supporting climate adaptation strategies and water resource management, particularly in anticipating spatially heterogeneous rainfall conditions during La Niña events.

## 2. Basic algorithm and extensions

### 2.1. Bayesian Analysis

Bayesian analysis is a statistical approach that utilizes Bayes' theorem to update information about model parameters based on the likelihood function and prior knowledge. The likelihood function is a function used to describe parameter information and is presented in the data and parameter functions [21]. In Bayesian analysis, this function is combined with past data as prior information. In other words, the posterior distribution is expressed by the ratio between the joint density function of the parameters obtained from the likelihood function, the prior distribution, and the posterior marginal function [21, 22]. The main advantages of Bayesian analysis lie in its ability to produce posterior distributions that reflect parameter uncertainty more comprehensively, its flexibility in handling complex models, and its provision of intuitive results in the form of parameter probabilities. In addition, this approach is very useful in hierarchical and spatial modeling because it is able to accommodate nested data structures and inter-location dependencies [23].

## 2.2. Conditional Autoregressive Model

CAR models are one approach in spatial statistics used to analyze data with spatial autocorrelation between locations that developed by Besag in 1974 [24]. This model is based on the assumption that the value of a variable at a particular location is influenced by the value of the same variable in surrounding locations. CAR belongs to the Markov Random Field (MRF) class, where dependencies between locations are expressed through conditional distributions, rather than overall marginal distributions.

Each location  $i$  has a conditional distribution determined by the values in its neighboring locations. In general, the conditional distribution is written as [25]:

$$Y_i | Y_{-i} \sim \mathcal{N} \left( \sum_{j \in \delta_i} \beta_{ij} Y_j, \tau_i^2 \right)$$

with  $Y_i$  being the value at location  $i$ ,  $Y_{-i}$  being the value at another location,  $\delta_i$  denotes the set of neighbors of location  $i$ ,  $\beta_{ij}$  is the spatial connectivity parameter, and  $\tau_i^2$  is the error variance.

Spatial relationships in CAR are modeled using a spatial weight matrix  $\mathbf{W}$ . This matrix defines the neighbors of each location and the weight of their influence. This representation allows CAR to capture spatial variation flexibly, both in terms of direct neighborhood and distance-based weights.

Spatial relationships in the CAR model are represented through a spatial weight matrix  $\mathbf{W} = (w_{ij})$ , which was constructed based on *queen contiguity*. Two regions are defined as neighbors if they share either a common boundary or a common vertex [27].

Specifically, the elements of the spatial weight matrix are defined as:

$$w_{ij} = \begin{cases} 1, & \text{if regions } i \text{ and } j \text{ are adjacent,} \\ 0, & \text{otherwise,} \end{cases}$$

with  $w_{ii} = 0$  for all regions.

The spatial weight matrix was not row-normalized, following the standard CAR specification implemented in the CARBayesST framework, where spatial dependence is governed by the adjacency structure and model-specific constraints, such as the sum-to-zero constraint in the spatial dependence parameter in Leroux-type CAR and ICAR models

## 2.3. Intrinsic Conditional Autoregressive Model

The Intrinsic Conditional Autoregressive (ICAR) model is one of the earliest and most commonly used spatial prior structures in Bayesian spatial statistics, originally proposed by Besag [24]. The ICAR model is designed to capture spatial dependence by assuming that the spatial random effect at a given location is conditionally dependent on the random effects of its neighboring locations.

Let  $u_i$  denote the spatial random effect associated with area  $i$ . Under the ICAR specification, the conditional distribution of  $u_i$  given the random effects of neighboring areas is defined as [28]:

$$u_i | u_{-i} \sim \mathcal{N} \left( \frac{1}{n_i} \sum_{j \in \delta_i} u_j, \frac{\sigma^2}{n_i} \right),$$

where  $\delta_i$  represents the set of neighboring areas of region  $i$ ,  $n_i$  denotes the number of neighbors, and  $\sigma^2$  is the variance parameter controlling the overall spatial variability. This formulation implies that the expected value of the spatial effect in a given area is equal to the average of the spatial effects in its neighboring areas, thereby inducing spatial smoothing.

A key characteristic of the ICAR model is that it assumes a fixed and maximal degree of spatial dependence, meaning that the strength of spatial autocorrelation is not governed by an explicit spatial dependence parameter. As a result, the joint prior distribution of the spatial random effects is improper. To ensure model identifiability, constraints such as a sum-to-zero restriction on the spatial random effects are typically imposed.

#### 2.4. Bayesian Leroux Conditional Autoregressive Model

Leroux CAR developed to overcome the intrinsic limitations of CAR (ICAR), which often produce improper priors and difficult-to-control spatial dependence. The Leroux formulation [4] introduces a spatial smoothing parameter  $\rho \in [0, 1]$  that smoothly interpolates between a model without spatial dependence ( $\rho = 0$ ) and pure ICAR ( $\rho = 1$ ). Thus, it provides a proper Gaussian Markov Random Field (GMRF) prior for spatial random effects that is stable in inference, particularly in small area scenarios or sparse data.

In regional rainfall modeling, such as rainfall in East Java, atmospheric continuity and orographic effects cause rainfall values in one region to be influenced by neighboring regions. Leroux CAR utilizes the spatial weight matrix  $W$  to represent this proximity structure. Thus, spatial variation in residuals or latent fields can be modeled explicitly, resulting in more realistic rainfall pattern estimates than approaches that ignore spatial autocorrelation.

The spatial regression model with Leroux CAR random effects for rainfall response  $y = (y_1, \dots, y_n)^\top$  in  $n$  areas can be written as:

$$y = X\beta + \phi + \varepsilon, \quad \varepsilon \sim \mathcal{N}(0, \sigma^2 I_n), \quad \phi \sim \mathcal{N}(0, \tau^2 Q(\rho, W)^{-1}),$$

where  $X$  is the covariate matrix (e.g., elevation, distance to coast, monsoon/ENSO index, temperature, humidity, land cover),  $\beta$  is the vector of fixed effects,  $\phi$  denotes spatial random effects, and  $\varepsilon$  represents the nugget effect (i.i.d. noise). The Leroux precision matrix is defined as:

$$Q(\rho, W) = \rho(D - W) + (1 - \rho)I_n,$$

where  $D = \text{diag}(W\mathbf{1})$  is the degree matrix of neighborhood structure. When  $\rho = 0$ , the random effects  $\phi$  become i.i.d. (no spatial correlation); when  $\rho = 1$ , the precision structure reduces to the ICAR form. The parameters to be estimated include  $\beta$  as covariate effect,  $\tau^2$  as variance of structured spatial effect, and  $\rho$  as spatial dependence intensity.

The Bayesian Leroux CAR formulation is obtained by placing priors on the model parameters as follow [26]:

$$\beta \sim \mathcal{N}(\mu_\beta, \Sigma_\beta), \quad \tau^2 \sim \text{Inv-Gamma}(a_\tau, b_\tau), \quad \rho \sim \text{Unif}(0, 1),$$

Together with the Leroux prior for the spatial random effects  $\phi$  as defined earlier. Assuming normality of  $\varepsilon$ , the full conditional distributions for  $\beta$ ,  $\phi$ ,  $\sigma^2$ , and  $\tau^2$  are mostly conjugate, and can therefore be updated using Gibbs sampling steps. The spatial dependence parameter  $\rho$  is typically non-conjugate, and is updated using Metropolis–Hastings or slice sampling schemes.

For rainfall prediction, the Bayesian inference scheme yields the posterior predictive distribution

$$p(y_{\text{new}} \mid y),$$

which describes rainfall at the same areas or, when combined with geostatistical models, at unobserved locations. This predictive distribution naturally provides measures of uncertainty, such as predictive standard deviations or 95% credible intervals, which are crucial for decision-making in food security, reservoir operations, and flood/drought risk mitigation.

#### 2.5. Goodness of Fit of Bayesian Method

In Bayesian analysis, goodness of fit and model convergence are typically evaluated through MCMC simulation results. Some commonly used tools include trace plots, density plots, autocorrelation plots, and credible intervals [21]. Trace plots display the parameter values generated at each MCMC iteration. A good chain will appear stable without a clear upward or downward trend. This plot helps to check whether the chain has reached stationarity and is mixing well. Density plots describe the posterior distribution estimates of a parameter. If MCMC is run with multiple chains, the distribution results from each chain should overlap. This indicates that all chains are converging to the same posterior distribution, suggesting that the model has converged. The Autocorrelation Plot is used to see the extent to which MCMC samples at a given iteration still depend on previous iterations. A good MCMC chain should show low correlation between samples. If the correlation is high, it means that the exploration of the posterior space is less efficient, resulting in a small effective sample size (ESS). Credible Interval states the range

of parameter values with a certain probability based on the posterior distribution. For example, a 95% credible interval indicates that there is a 95% probability that the parameter is within that interval. This interval is a measure of the uncertainty of the parameter estimate.

RMSE is often used as a measure of the performance of Bayesian models in predicting data. RMSE is calculated from the root of the average square difference between the observed value and the predicted value. A smaller RMSE value indicates that the model provides more accurate predictions. In the context of rainfall forecasting, RMSE provides important information about how close the model's rainfall predictions are to the actual observed rainfall values.

## 2.6. Study Area and Data Source

This research was conducted in East Java Province, Indonesia, which is geographically located between 111°0'–114°4' East Longitude and 7°12'–8°48' South Latitude. East Java has a diverse topography, ranging from coastal areas and lowlands to mountainous regions. These geographical characteristics lead to significant spatial and temporal variation in rainfall distribution across the province. Rainfall in East Java is influenced by global climate drivers such as *El Niño–Southern Oscillation (ENSO)*, the Asian–Australian monsoon [29], as well as local factors such as elevation, humidity, temperature, wind direction and speed, and cloud cover. The heterogeneity of this region makes East Java a suitable study area for spatial rainfall analysis using the BCAR model, which explicitly accounts for spatial dependence across districts and municipalities.

Although large-scale climate indices (e.g., ENSO) and physiographic variables such as elevation are known to play an important role in regulating rainfall patterns in East Java, these factors were not explicitly included as covariates in the present study. This decision was primarily motivated by considerations of data availability, spatial consistency at the district and municipal levels, and the need to maintain uniform spatial resolution across all explanatory variables. Consequently, the analysis focuses on modeling spatial variability in rainfall associated with locally observed climatic conditions.

The data used in this study came from two main sources, namely the Meteorology, Climatology, and Geophysics Agency (BMKG) and ERA5 reanalysis data from the European Centre for Medium-Range Weather Forecasts (ECMWF). The data used was monthly rainfall during the 2022 and 2023 rainy seasons, which coincided with the La Niña phase. The La Niña phase is used as a general climatological context, not as an explicit predictor variable in the model. The rainy season in East Java is divided into two sub-periods, namely the transition to rainy seasons (September–November) and the core rainy season (December–February). This division of periods allows for a more detailed analysis of rainfall variations, both those influenced by global climate phenomena and regional conditions. The division of data into two seasonal sub-periods was done to simplify spatial analysis, but this approach ignores intra-seasonal and inter-monthly temporal dynamics. Therefore, the analysis in this study focuses on modeling historical spatial patterns, rather than for the purpose of rainfall forecasting.

This study employs one dependent variable (rainfall) and five independent variables (humidity, temperature, wind direction, wind speed, and cloud cover) [30]. The selection of five climate variables in this study was based on practical and methodological considerations, namely the availability of complete data and spatial consistency between administrative regions during the observation period. The operational definitions and units of the variables are presented in Table 1.

## 2.7. Simulation Study

A simulation study was conducted to evaluate the performance of the BCAR model in estimating spatial regression parameters. Simulation provides a powerful framework for evaluating model performance by allowing researchers to control data-generating processes. By manipulating key parameters and generating synthetic datasets, analysts can systematically compare their model's estimation results against the known, true parameters. This direct comparison facilitates a rigorous assessment of model accuracy, leveraging metrics like bias measures to quantify and evaluate the precision of the estimated parameters. This method is particularly valuable for understanding a model's robustness and efficiency under various controlled conditions. This approach is important because it provides an overview of the reliability of the method used when applied to real data with complex spatial characteristics.

Table 1. Research Variables

No	Variable	Notation	Definition	Unit
1	Rainfall	$Y$	The amount of rainwater that falls to the earth's surface within a specific time period.	mm
2	Temperature	$X_1$	A measure of the degree of hotness or coldness of the air at a certain location.	°C
3	Humidity	$X_2$	The percentage of water vapor in the air compared to the maximum amount that the air can hold at a given temperature.	%
4	Wind Speed	$X_3$	The rate of air movement at a specific location	km/h
5	Wind Direction	$X_4$	The direction from which the wind blows, usually expressed in degrees or compass points.	Degree
6	Cloud Cover	$X_5$	The percentage of the sky covered by clouds, which affects solar radiation intensity and precipitation potential.	%

The simulation process was carried out by generating data with a spatial structure similar to the original data, using a spatial weight matrix obtained from 38 districts/cities in East Java. The explanatory variables were generated following a normal distribution with specific mean and standard deviation parameters, adjusted to the statistical summary of the real data. The spatial effects were generated based on the existing neighborhood structure, so that the spatial patterns in the simulation data continued to represent empirical conditions.

Furthermore, the simulated data were used to estimate the BCAR model using the Bayesian method. This process was repeated 200 times to obtain a stable evaluation measure. From each replication, the estimated parameters included the regression coefficient  $\beta$ , variance  $\tau^2$ , and spatial autocorrelation parameters  $\rho$  for Leroux BCAR. The estimation results are then compared with the actual values through bias and RMSE calculations, providing an overview of how close the estimation results are to the population parameters.

With this simulation design, the performance of the best model based RMSE can be comprehensively assessed. If the bias and RMSE obtained are relatively small, then the model can be said to be able to capture spatial relationships well. Conversely, if a large bias is found, this indicates that the model needs to be further developed, either through adjustment of assumptions or the use of alternative approaches. Thus, this simulation study serves as a methodological validation stage before applying the model to rainfall data in East Java.

### 3. Experimental Results

#### 3.1. Descriptive Statistics

Figure 2a and Figure 2b are the spatial distribution of monthly rainfall in East Java during two different seasonal periods, namely the transition season (Sep–Nov) and the rainy season (Dec–Feb). During the transition season (panel a), rainfall patterns vary considerably between regions, with most areas experiencing moderate to low rainfall intensity (around 100–300 mm). This variation reflects the transition from the dry season to the rainy season, when atmospheric conditions are not yet fully stable. Some southern and western regions begin to experience higher rainfall compared to the northern and eastern parts, which are still relatively dry. This is consistent with the Asian monsoon pattern, which begins to actively bring moist air masses from the Indian Ocean to southern Indonesia.

During the rainy season (panel b), almost all of East Java experienced a significant increase in rainfall. Rainfall intensity is higher and more evenly distributed, especially in the southern and central regions, with some areas reaching more than 400 mm per month. This pattern confirms the role of the western monsoon in bringing large amounts of water vapor, resulting in high rainfall in most areas. Areas with mountainous topography, such as Malang and its surroundings, appear to receive higher rainfall due to orographic effects that enhance the condensation process.



The La Niña phenomenon that occurred during the study period also strengthened rainfall intensity, both in the transition season and the rainy season. La Niña is characterized by cooler sea surface temperature anomalies in the central and eastern Pacific Ocean, which have an impact on increasing water vapor flow from the Pacific Ocean to the Indonesian maritime region. As a result, the potential for rainfall in East Java increased above normal conditions, with a wider spatial distribution. The impact of La Niña was clearly seen during the rainy season, where rainfall was not only higher but also more evenly distributed across almost the entire region.

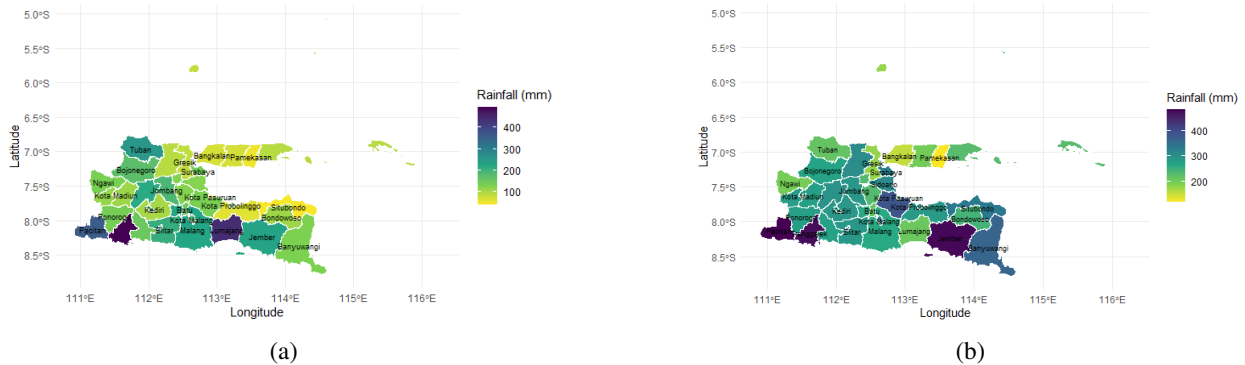


Figure 1. Monthly Rainfall in East Java During: (a) Transition Season (Sep–Nov); (b) Rainy Season (Dec–Feb).

To further investigate the spatial dependency of rainfall, the Moran's I test under randomization was performed. The results yield a Moran's I value of 0.2404, with an expected value of  $-0.0270$  and a variance of 0.0156. The standard deviate was 2.1439, corresponding to a p-value of 0.0160. These findings suggest a statistically significant positive spatial autocorrelation, implying that districts with higher rainfall values are more likely to be adjacent to districts with similarly high rainfall values, and vice versa.

Next, a multicollinearity analysis was conducted to ensure that there were no strong linear relationships between the independent variables used in the model. The test was performed using the Variance Inflation Factor (VIF) value. The results showed that the temperature variable had a VIF value of 7.30; humidity 3.80; wind speed 1.92; wind direction 1.77; and cloud cover 5.94. In general, all VIF values were below the threshold of 10, which is commonly used as an indicator of serious multicollinearity. This indicates that the climate variables used in this study are relatively independent of each other and do not cause high correlation problems that could affect the stability of model parameter estimates. However, the VIF values for the temperature (7.30) and cloud cover (5.94) variables show a higher correlation tendency than the other variables, but are still within acceptable tolerance limits. Although all VIF values are below the conventional threshold of 10, the relatively higher VIF observed for temperature and cloud cover suggests the presence of moderate collinearity within the set of climatic covariates.

### 3.2. Model Estimation: Bayesian Leroux CAR

The estimation of rainfall patterns in East Java was carried out using the BCAR model, which explicitly accounts for spatial dependence across districts. This approach is particularly suitable for climatological data where rainfall in one area is likely to be correlated with its neighboring regions. Model estimation was implemented using MCMC with the following settings: one chain, 500,000 iterations, a burn-in of 40,000, and thinning of 100. These specifications ensure that the Markov chains converge and produce stable posterior samples, thus providing reliable estimates of the model parameters that shows in Table 2.

During the rainy season, the analysis showed that while most climate variables have wide credible intervals and aren't statistically significant. The spatial dependence parameter  $\hat{\rho}$  was estimated at 0.398, suggesting a moderate spatial autocorrelation in rainfall. The model performed adequately, as indicated by its DIC of 447.60 and LMPL of -226.64.

In the transition to rainfall season, the results differ slightly. Cloud cover emerges as a significant predictor of rainfall with a posterior mean of 14.0154 (95% CI: 1.5468–26.4426), implying that greater cloud cover is strongly

Table 2. Summary of Bayesian Leroux CAR Model Results for Rainfall in East Java

Parameter	Rainy Season	95% CI	Transition Season	95% CI
Intercept	-111.847	(-2138.18, 1900.92)	-2591.24	(-4700.36, -533.05)
Temperature ( $\hat{\beta}_1$ )	-5.365	(-39.73, 28.71)	25.912	(-9.14, 61.49)
Humidity ( $\hat{\beta}_2$ )	7.014	(-5.67, 19.63)	12.360	(-0.90, 25.49)
Wind Speed ( $\hat{\beta}_3$ )	3.347	(-9.86, 16.61)	11.760	(-1.66, 25.11)
Wind Direction ( $\hat{\beta}_4$ )	-0.157	(-0.74, 0.39)	0.068	(-0.49, 0.63)
Cloud Cover ( $\hat{\beta}_5$ )	-0.206	(-12.59, 12.04)	14.015	(1.55, 26.44)
$\hat{\tau}^2$	1.110	(0.45, 2.57)	1.106	(0.46, 2.61)
$\hat{\rho}$	0.398	(0.02, 0.92)	0.401	(0.02, 0.92)
DIC		447.60		449.13
LMPL		-226.64		-227.92

associated with increased rainfall. Temperature, humidity, and wind speed also show positive but statistically uncertain effects. The spatial dependence parameter ( $\hat{\rho}$ ) remains consistent at 0.4008 (95% CI: 0.0152–0.9195), confirming similar spatial dependence across seasons. Model fit indices yield a DIC of 449.13 and LMPL of  $-227.92$ , comparable to the rainy season. The Bayesian Leroux CAR model successfully captures the spatial correlation in rainfall across East Java. Although not all climatic predictors are statistically significant, the stable estimation of  $\hat{\rho}$  across both seasons highlights the importance of spatial effects in explaining rainfall variability. This confirms the utility of Bayesian CAR models as a robust methodological framework for analyzing spatial climatological data.

The posterior summaries in Table 2 reveal substantial uncertainty in several regression parameters, particularly for the intercept and temperature during the rainy season, where the 95% credible interval spans a wide and implausible range. In a Bayesian spatial framework, such moderate collinearity can be amplified by the inclusion of spatial random effects, leading to partial confounding between fixed effects and the latent spatial component. This interaction reduces parameter identifiability and inflates posterior uncertainty, even when classical multicollinearity diagnostics do not indicate a severe problem.

The wide credible intervals observed for several climatic variables, particularly temperature and cloud cover in the rainy season, therefore likely reflect competition between the covariates and the spatial random effects in explaining rainfall variability. This phenomenon is consistent with previous findings in spatial Bayesian regression, where spatial smoothing can absorb variation that might otherwise be attributed to correlated predictors. As a result, while individual parameter estimates exhibit high uncertainty, the spatial dependence parameter remains stable and well-identified across both seasons, with posterior means of approximately 0.40. This contrast highlights that spatial structure plays a more dominant and robust role in explaining rainfall variability in East Java than individual point-in-time climatic covariates.

The implausibly wide credible intervals for the intercept, especially during the transition season, suggest that the overall mean rainfall level is weakly identified once spatial effects and correlated predictors are accounted for. This reinforces the interpretation that the model is more reliable for capturing spatial patterns rather than for precise estimation of individual regression coefficients. Consequently, the inference from this model should emphasize spatial dependence and predictive performance rather than the statistical significance of specific climatic variables.

### 3.3. Model Estimation: Bayesian ICAR

The results of the Bayesian ICAR model estimation (Table 3) show that during the rainy season, a positive intercept value indicates that the base rainfall is relatively high when all covariates are at their mean values. The temperature variable has a negative coefficient, indicating that an increase in temperature tends to decrease rainfall, although the fairly wide 95% credible interval range, which still includes values close to zero, indicates relatively high estimation uncertainty. Conversely, humidity and wind speed show a positive effect on rainfall, which is consistent with atmospheric physical processes in which more humid air and stronger wind dynamics contribute to precipitation



formation. Wind direction does not show a significant effect, while cloud cover has a negative coefficient with a relatively wide confidence interval, indicating a statistically weak relationship in the model.

Table 3. Summary of Bayesian ICAR Model Results for Rainfall in East Java

Parameter	Rainy Season	95% CI	Transition Season	95% CI
Intercept	1161.644	(-739.800, 3058.627)	-1463.623	(-3399.280, 438.027)
Temperature ( $\hat{\beta}_1$ )	-26.538	(-59.116, 6.574)	6.695	(-25.458, 39.438)
Humidity ( $\hat{\beta}_2$ )	1.082	(-10.306, 12.522)	7.225	(-4.527, 18.898)
Wind Speed ( $\hat{\beta}_3$ )	17.469	(2.543, 32.045)	26.439	(12.103, 41.376)
Wind Direction ( $\hat{\beta}_4$ )	-0.073	(-0.555, 0.406)	0.187	(-0.294, 0.674)
Cloud Cover ( $\hat{\beta}_5$ )	-6.908	(-18.128, 4.358)	7.761	(-3.517, 18.997)
$\hat{\tau}^2$	1.241	(0.488, 3.024)	1.259	(0.489, 3.144)
DIC		437.298		438.301
LMPL		-222.830		-222.47

During the transition season, a slightly different pattern is observed. Temperature again shows a negative effect on rainfall, while humidity and wind speed have a stronger positive effect compared to the rainy season, as reflected in the larger coefficient values. This can be interpreted to mean that during the transition season, rainfall variation is more sensitive to atmospheric dynamics than to stable seasonal conditions. However, some variables, such as wind direction and cloud cover, still show high uncertainty, as indicated by wide credible intervals that include zero. This indicates that the influence of these variables is not spatially or temporally consistent during the transition period.

The width of the credible intervals for several parameters, both in the rainy season and the transition season, indicates considerable estimation uncertainty. This condition can be attributed to moderate multicollinearity between covariates, as reflected in the VIF values. These VIF values indicate that there is moderate correlation between explanatory variables, causing the information carried by each covariate to overlap. As a result, although the coefficient signs can still be interpreted substantively, the accuracy of the estimates decreases and produces wider credible intervals.

In the context of Bayesian ICAR spatial modeling, this phenomenon is also influenced by the presence of spatial random effects that absorb some of the data variation. The ICAR spatial effect serves to capture the dependence between neighboring areas, so that the contribution of covariates becomes relatively smaller and less certain when there is correlation between explanatory variables. Therefore, even though the ICAR model is able to improve the spatial dependency structure and reduce residual autocorrelation, the covariate estimation results still need to be interpreted carefully, especially when the credible interval is wide and the VIF is at a moderate level.

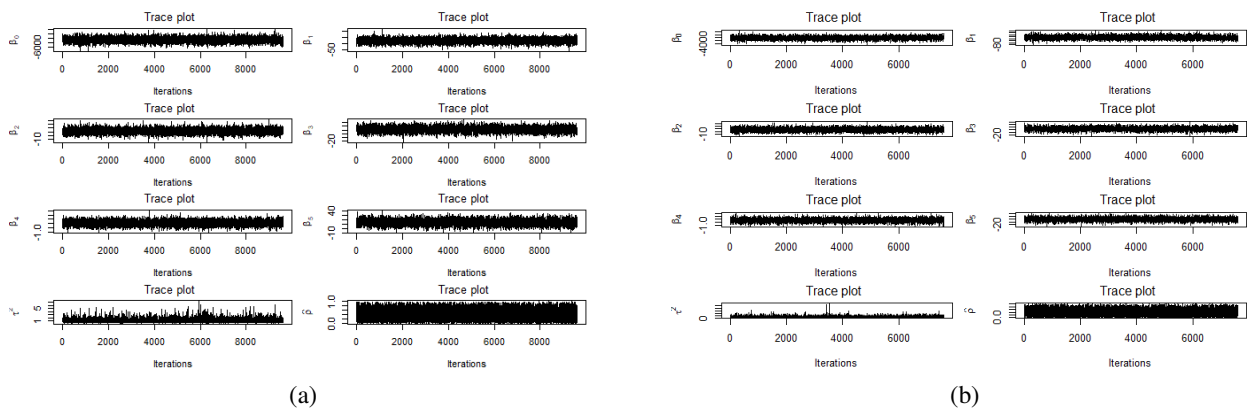


Figure 2. Trace Plots of All BCAR Model Parameters in: (a) Transition Season (Sep–Nov); (b) Rainy Season (Dec–Feb).

### 3.4. Goodness of Fit of the Bayesian CAR Model

Model performance was evaluated through the convergence diagnostics of the MCMC simulation in Figure 2a and Figure 2b, namely trace plots for all parameters ( $\hat{\beta}_0, \dots, \hat{\beta}_5, \hat{\tau}^2, \hat{\rho}$ ). The trace plots show stable fluctuations around their mean values without visible trends, indicating that the MCMC chains have reached convergence.

Specifically, the posterior distribution of  $\hat{\beta}_2$  (temperature) and  $\hat{\beta}_3$  (wind direction) are centered on positive values, indicating a significant positive association with rainfall. In contrast,  $\hat{\beta}_1$  (humidity) and  $\hat{\beta}_4$  (wind speed) tend to be negative, while  $\hat{\beta}_5$  (cloud cover) fluctuates around zero with higher uncertainty. The spatial dependence parameter  $\hat{\rho}$  is concentrated between 0.3 and 0.6, implying a moderate level of spatial autocorrelation in rainfall data. Meanwhile,  $\hat{\tau}^2$  remains positive with a relatively dispersed posterior, reflecting unexplained structured spatial heterogeneity.

### 3.5. Prediction Results

Based on Figure 3a and Figure 3b, the spatial predictions of monthly rainfall in East Java using the Leroux BCAR model reveal distinct seasonal characteristics. During the transition season, as shown in Figure 3(a), rainfall exhibits considerable spatial heterogeneity. Higher rainfall intensities are predicted in the central and eastern parts of East Java, particularly in regions such as Malang, Blitar, and Bondowoso. This pattern is closely associated with mountainous topography, where orographic effects enhance precipitation. In contrast, northern coastal areas such as Surabaya, Gresik, and Tuban are characterized by relatively lower rainfall, which is consistent with the drier conditions typically observed in coastal regions during the transition season. These results confirm that the transition season is marked by an uneven spatial distribution of rainfall, with pronounced contrasts between wetter inland areas and drier coastal zones. During the rainy season (December–February), the Leroux BCAR model predicts a much more homogeneous spatial pattern of rainfall, as illustrated in Figure 3(b). High rainfall intensities dominate across nearly all districts and cities in East Java, as indicated by the widespread presence of darker colors on the map. This spatial uniformity reflects the defining characteristics of the rainy season in tropical monsoon regions, where large-scale atmospheric processes and abundant moisture supply reduce spatial contrasts in precipitation.

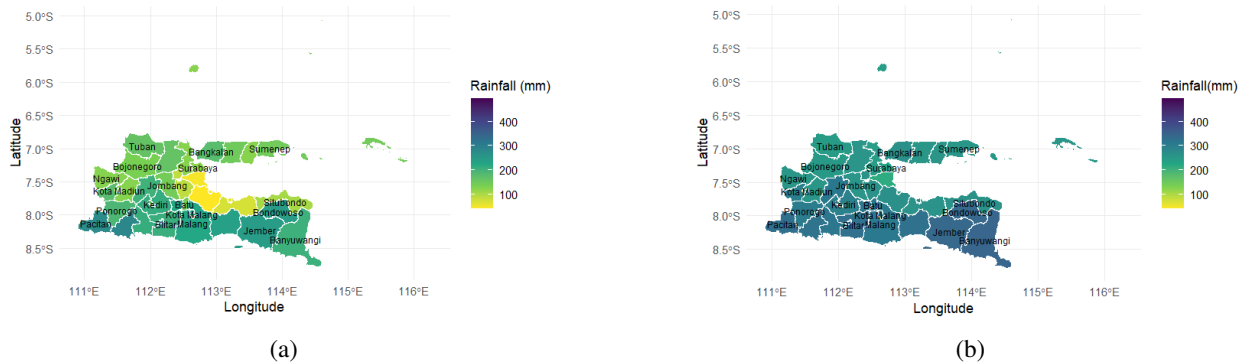


Figure 3. Prediction of Monthly Rainfall using Leroux BCAR Model in East Java During: (a) Transition Season (Sep–Nov); (b) Rainy Season (Dec–Feb).

Figure 4a and Figure 4b present the corresponding monthly rainfall predictions obtained using the ICAR model. While the general spatial patterns remain broadly consistent with those of the Leroux BCAR model, the ICAR results display sharper local contrasts. In the transition season (Figure 4(a)), differences between wetter mountainous areas in the southern and central regions and the drier northern coastal zones appear more pronounced. This behavior reflects the structure of the ICAR model, in which the spatial dependence is entirely governed by the neighborhood structure without a global spatial smoothing parameter, making the model more sensitive to local spatial variations. In the rainy season (Figure 4(b)), rainfall remains generally high and spatially widespread across

East Java; however, the ICAR model still preserves a higher degree of residual spatial variability compared to the Leroux BCAR model. Certain regions maintain noticeably higher or lower predicted rainfall than their neighbors, suggesting that the ICAR model retains localized spatial heterogeneity even under relatively uniform seasonal conditions.

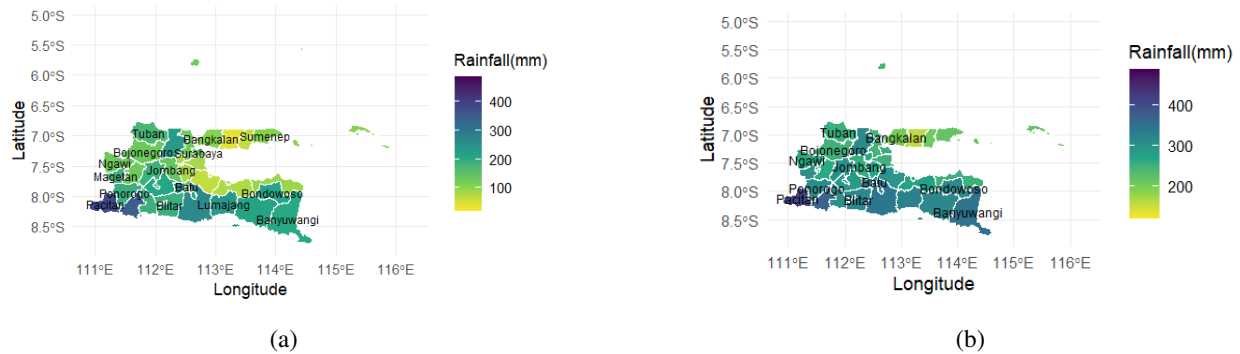


Figure 4. Prediction of Monthly Rainfall using Leroux BCAR Model in East Java During: (a) Transition Season (Sep–Nov); (b) Rainy Season (Dec–Feb).

These qualitative differences between the Leroux BCAR and ICAR models are supported by the quantitative evaluation based on the RMSE. As shown in Table 4, the ICAR model yields substantially lower RMSE values, namely 62.0 mm for the transition season and 60.1 mm for the rainy season, indicating superior predictive accuracy relative to both the Leroux BCAR and the non-spatial linear regression model. In contrast, the Leroux BCAR model produces higher RMSE values of 73.5 mm and 73.9 mm for the transition and rainy seasons, respectively, reflecting a tendency toward overestimation of monthly rainfall.

Despite its higher RMSE, the Leroux BCAR model provides smoother and more stable spatial predictions, which can be advantageous for regional-scale rainfall mapping and interpretation. Compared to the linear regression model, which yields RMSE values of approximately 72–73 mm in both seasons, both spatial models demonstrate the importance of accounting for spatial dependence in rainfall prediction. Overall, these results highlight a trade-off between predictive accuracy and spatial smoothness: the ICAR model excels in capturing local variability and minimizing prediction error, whereas the Leroux BCAR model offers more spatially coherent representations of monthly rainfall patterns across East Java.

From a practical perspective, the magnitude of the RMSE values obtained in this study must be interpreted in the context of monthly rainfall variability. An RMSE in the range of 60–75 mm implies that, on average, the model predictions deviate from the observed monthly rainfall by approximately 60 to 75 mm. For monthly rainfall data, this level of error is not unusually high, particularly in tropical regions such as East Java where monthly rainfall can vary substantially, often exceeding 200–400 mm during the rainy season. According to operational rainfall classifications commonly used by meteorological agencies, including BMKG, a deviation of this magnitude generally remains within one rainfall category (e.g., low to moderate or moderate to high), suggesting that the models still provide reasonably informative predictions at the monthly scale.

The results of this study have practical implications for water resource management and flood risk assessment in East Java, as the spatial rainfall patterns identified by the BCAR and ICAR models can support regional planning, reservoir operation, and flood preparedness, particularly in areas consistently predicted to experience higher rainfall. However, the interpretation of the results must consider several limitations. The moderate multicollinearity among climate covariates and potential spatial confounding contribute to wide credible intervals and elevated parameter uncertainty, limiting the reliability of covariate-specific inferences. In terms of predictive performance, the RMSE values—while still acceptable for monthly rainfall modeling in a tropical region with high variability—indicate that prediction errors remain non-negligible, especially for flood-sensitive areas. The lower RMSE achieved by the ICAR model suggests superior predictive accuracy compared to the Leroux BCAR model,

Table 4. RMSE of BCAR Model by Season

Season	Model	RMSE
Transition Season (Sep–Nov)	Linier Regression	73.6
Rainy Season (Dec–Feb)	Linier Regression	72.9
Transition Season (Sep–Nov)	ICAR	62.0
Rainy Season (Dec–Feb)	ICAR	60.1
Transition Season (Sep–Nov)	BCAR	73.5
Rainy Season (Dec–Feb)	BCAR	73.9

making ICAR more suitable for operational rainfall estimation, whereas the Leroux model remains valuable for capturing smoother regional spatial structures. Future studies should incorporate additional explanatory variables and adopt spatio-temporal frameworks to further reduce uncertainty and enhance the applicability of spatial rainfall models for hydrometeorological risk management.

### 3.6. Result of Simulation Study

The simulation study was conducted to evaluate the stability and consistency of the parameter estimates obtained from the ICAR model as the best model in this case. This step is important to determine whether the estimates derived from secondary data are consistent with the distribution of estimates obtained through repeated simulations.

Table 5. One-sample t-test Results: Comparison Between Secondary Data Estimates and Simulation Means for ICAR Models

Parameter	Season	Secondary	Mean Sim.	SD Sim.	<i>t</i> statistic	<i>p</i> -Value	Decision
$\hat{\beta}_0$ (Intercept)	Rainy	-111.847	-112.896	32.029	0.463	0.644	Not Sig.
$\hat{\beta}_1$ (Temp)	Rainy	-5.365	-5.311	0.783	-0.974	0.331	Not Sig.
$\hat{\beta}_2$ (Humidity)	Rainy	7.014	6.998	0.222	0.982	0.327	Not Sig.
$\hat{\beta}_3$ (Wind Spd)	Rainy	3.347	3.351	0.358	-0.134	0.894	Not Sig.
$\hat{\beta}_4$ (Wind Dir)	Rainy	-0.157	-0.156	0.014	-1.180	0.239	Not Sig.
$\hat{\beta}_5$ (Cloud)	Rainy	-0.206	-0.197	0.205	-0.611	0.542	Not Sig.
$\hat{\tau}^2$	Rainy	1.110	1.184	0.698	-1.503	0.134	Not Sig.
$\hat{\rho}$	Rainy	0.398	0.393	0.043	1.643	0.102	Not Sig.
$\hat{\beta}_0$ (Intercept)	Transition	-1463.623	-1476.620	65.425	0.043	0.966	Not Sig.
$\hat{\beta}_1$ (Temp)	Transition	6.695	6.372	1.158	-0.511	0.610	Not Sig.
$\hat{\beta}_2$ (Humidity)	Transition	7.225	7.750	0.570	1.088	0.279	Not Sig.
$\hat{\beta}_3$ (Wind Spd)	Transition	26.439	25.862	0.657	-0.864	0.389	Not Sig.
$\hat{\beta}_4$ (Wind Dir)	Transition	0.187	0.200	0.042	0.306	0.760	Not Sig.
$\hat{\beta}_5$ (Cloud)	Transition	7.761	7.628	0.368	-0.672	0.503	Not Sig.
$\hat{\tau}^2$	Transition	1.259	1.249	0.001	-0.756	0.452	Not Sig.

The simulation was carried out 200 times by generating datasets that follow the same structure as the secondary data. For each replication, parameter estimates were obtained, and the mean as well as the standard deviation were calculated. To compare the simulation results with the secondary data estimates, a one-sample test was applied with the following hypotheses:

$$H_0 : \mu = \theta, \quad H_1 : \mu \neq \theta$$

where  $\mu$  denotes the mean of the simulated estimates and  $\theta$  is the estimate obtained from the secondary data. The test statistic is given by:

$$t = \frac{\bar{X} - \theta}{s/\sqrt{n}}$$

with  $\bar{X}$  = mean of simulated estimates,  $s$  = standard deviation of simulation results,  $n = 200$  the number of simulations, and  $\theta$  = the estimate from secondary data. Decisions were made based on the  $p$ -value at a significance level of  $\alpha = 0.05$ .

The results of the comparison between simulated means and secondary data estimates are summarized in Table 5.

As presented in Table 5, all regression parameter estimations ( $\hat{\beta}_0 \dots \hat{\beta}_5$ ) as well as the spatial correlation parameter estimation ( $\hat{\rho}$ ) and variance parameter ( $\hat{\tau}^2$ ) show no significant differences between the secondary data estimates and the simulation means, for both rainy and transition seasons. This indicates that the ICAR Model has an unbiased estimator.

#### 4. Conclusion

This study applies BCAR models to estimate and map rainfall patterns in East Java while explicitly accounting for spatial dependence between regions. Two BCAR specifications were evaluated, namely the Leroux CAR and the ICAR models. The results indicate that, although most climatic covariates such as temperature, humidity, and wind-related variables exhibit wide credible intervals and lack statistical significance, spatial effects play a crucial role in explaining rainfall variability. In particular, the spatial dependence parameter in the Leroux CAR model remains stable at approximately  $\rho = 0.39$ – $0.40$  across both the transition and rainy seasons, confirming the presence of moderate and persistent spatial autocorrelation. During the transition season, cloud cover emerges as a significant positive predictor of rainfall, highlighting its importance in the early phase of monsoon development.

Model comparison based on predictive performance reveals that the ICAR model consistently outperforms the Leroux CAR and non-spatial linear regression models in terms of RMSE. The ICAR model yields the lowest RMSE values for both the transition season (62.0 mm) and the rainy season (60.1 mm), indicating superior predictive accuracy for monthly rainfall. In contrast, the Leroux CAR model produces higher RMSE values (approximately 73–74 mm), comparable to those obtained from the non-spatial linear regression. This suggests that, while the Leroux CAR model provides smoother and more interpretable spatial patterns through controlled spatial smoothing, it may attenuate local rainfall variability, leading to reduced predictive accuracy relative to the ICAR specification.

The robustness of the model is further supported by simulation results. The parameters estimated from simulated data were shown to be unbiased, with their values closely matching the parameters derived from the secondary data. This outcome confirms that the Bayesian MCMC estimation procedure is not only stable but also produces reliable estimates for the spatial analysis of climatological data.

Despite these strengths, several limitations must be acknowledged. First, the relatively wide credible intervals observed for the intercept and several covariates indicate potential identifiability issues, which are likely related to moderate-to-high multicollinearity among the climatic variables, as reflected by VIF values are moderate. Such collinearity, particularly when combined with spatial random effects, can inflate posterior uncertainty and weaken inferential conclusions. Second, although the RMSE values are not unusually high for monthly rainfall in a tropical region with substantial variability, they nonetheless suggest that important sources of variation remain unexplained, especially local extremes and seasonal dynamics.

Future research should therefore prioritize the integration of additional explanatory variables, including large-scale climate indicators (e.g., ENSO-related indices), topographic characteristics, and-use factors, and interaction effect to reduce residual uncertainty and spatial confounding. Extending the analysis to a fully spatio-temporal Bayesian framework would also allow temporal dependence to be explicitly modeled, potentially improving predictive accuracy. While the ICAR model demonstrates superior performance in minimizing prediction error. and the Leroux CAR model offers more stable spatial interpretation, careful model selection remains essential depending on whether the primary objective is prediction accuracy or spatial inference in rainfall modeling for East Java.

## Acknowledgement

We would like to express our gratitude to Universitas Brawijaya for providing the financial support in DPP/SPP 2025. We are also thankful to the anonymous reviewers for the valuable comments and suggestions on the earlier draft paper.

## REFERENCES

1. W. Ploberger and P. C. B. Phillips, *Optimal Estimation Under Nonstandard Conditions*, SSRN Journal, 2010.
2. A. B. Badawaire, K. Ayinde, and S. O. Olanrewaju, *Development of a Robust Generalized Least Squares Liu Estimator to Address Some Basic Assumptions Violations in Linear Regression Model*, *Asian J. Prob. Stat.*, vol. 27, no. 5, pp. 12–31, 2025.
3. D. Lee, *A comparison of conditional autoregressive models used in Bayesian disease mapping*, *Spatial and Spatio-temporal Epidemiology*, vol. 2, no. 2, pp. 79–89, 2011.
4. B. G. Leroux, X. Lei, and N. Breslow, *Estimation of disease rates in small areas: a new mixed model for spatial dependence*, in *Statistical models in epidemiology, the environment, and clinical trials*, Springer, pp. 179–191, 2000.
5. R. Van De Schoot, *Bayesian statistics and modelling*. *Nat Rev Methods Primers*, vol. 1, no. 1, p. 1, 2021.
6. N. Iriawan, S. Astutik, and D. D. Prastyo, *Markov Chain Monte Carlo–Based Approaches for Modeling the Spatial Survival with Conditional Autoregressive (CAR) Frailty*, *International Journal of Computer Science and Network Security*, vol. 10, no. 12, pp. 211–216, 2010.
7. M. S. Pathan, J. Wu, Y. H. Lee, J. Yan, and S. Dev, *Analyzing the Impact of Meteorological Parameters on Rainfall Prediction*, in 2021 IEEE USNC-URSI Radio Science Meeting (Joint with AP-S Symposium), Singapore, IEEE, Singapore, pp. 100–101, 2021.
8. S. Astutik, N. Iriawan, G. Nair, Suhartono, and Sutikno, *Bayesian state space modeling for spatio-temporal rainfall disaggregation*, *International Journal of Applied Mathematics and Statistics*, vol. 37, no. 7, pp. 26–37, 2013.
9. M. Kumari, C. K. Singh, O. Bakimchandra, and A. Basistha, *Geographically weighted regression based quantification of rainfall–topography relationship and rainfall gradient in Central Himalayas*, *Intl Journal of Climatology*, vol. 37, no. 3, pp. 1299–1309, 2017.
10. S. Astutik, A. B. Astuti, N. S. Rahmi, D. Irsandy, and R. H. P. Y. Damayanti, *Generalized spatio temporal autoregressive rainfall-ens0 pattern in east java indonesia*, in *AIP Conference Proceedings*, AIP Publishing LLC, p. 020017, 2024.
11. R. E. Caraka, M. Ulhusna, B. D. Supatmanto, N. E. Goldameir, B. Hutapea, G. Darmawan, D. C. Novitasari, B. Pardamean, *Bayesian Hidden Markov modelling on East Java montly rainfall data*, in 2018 Indonesian Association for Pattern Recognition International Conference (INAPR), IEEE, pp. 75–79, 2018.
12. T. Holsclaw, A. M. Greene, A. W. Robertson, and P. Smyth, *A Bayesian Hidden Markov Model of Daily Precipitation over South and East Asia*, *Journal of Hydrometeorology*, vol. 17, no. 1, pp. 3–25, 2016.
13. S. Astutik, H. Pramoedyo, N. S. Rahmi, D. Irsandy, and R. H. P. Y. Damayanti, *Rainfall Data Modeling with Artificial Neural Networks Approach*, *Journal of Physics: Conference Series*, vol. 2123, no. 1, p. 012029, 2021.
14. V. Nourani, Ö. Kisi, and M. Komasi, *Two hybrid artificial intelligence approaches for modeling rainfall–runoff process*, *Journal of Hydrology*, vol. 402, no. 1–2, pp. 41–59, 2011.
15. A. Sarasa-Cabezuelo, *Prediction of rainfall in Australia using machine learning*, *Information*, vol. 13, no. 4, p. 163, 2022.
16. D. Teh, and T. Khan, *Types, definition and classification of natural disasters and threat level*, in *Handbook of disaster risk reduction for resilience: new frameworks for building resilience to disasters*, Springer International Publishing, Cham, pp. 27–56, 2021.
17. M. A. Hasibuan, I. A. Shidiq, H. A. Z. Asifin, Q. Sa'diyah, and Giarno, *The Quantifying the Relationship Between ENSO-Induced SST Anomalies and Rainfall Variability in East Java's Coastal Regions*, *Jurnal Geografi : Media Informasi Pengembangan dan Profesi Kegeografian*, vol. 21, no. 2, pp. 94–102, Dec. 2024.
18. J. R. Rodysill, J. M. Russell, M. Vuille, S. Dee, B. Lughino, and S. Bijaksana, *La Niña-driven flooding in the Indo-Pacific warm pool during the past millennium*, *Quaternary Science Reviews*, vol. 225, p. 106020, 2019.
19. F. Amin, A. K. Gupta, S. T. Ahmad, *Hydro-meteorological Extremes and Disasters: Integrated Risk, Remediation and Sustainability*, *Hydro-Meteorological Extremes and Disasters*, Springer, Singapore, pp. 3-15, 2022.
20. M. A. Haq, *CDLSTM: A novel model for climate change forecasting.*, *Computers, Materials & Continua*, vol. 71, no. 2, 2022.
21. J. K. Ghosh, M. Delampady, and T. Samanta, *An introduction to Bayesian analysis: theory and methods*, Springer, vol 725, 2006.
22. S. Astutik, A. B. Astuti, A. Efendi, D. Darmanto, D. Irsandy, and F. Y. D. A. S. Sanjayawati, *Analisis Bayesian: Teori dan Aplikasi dengan R*, Malang, Indonesia: Universitas Brawijaya Press, 2023.
23. A. E. Gelfand and S. Banerjee, *Bayesian Modeling and Analysis of Geostatistical Data*, *Annu. Rev. Stat. Appl.*, vol. 4, no. 1, pp. 245–266, Mar. 2017.
24. J. Besag, *Spatial interaction and the statistical analysis of lattice systems*, *Journal of the Royal Statistical Society: Series B (Methodological)*, vol. 36, no. 2, pp. 192–225, 1974.
25. C. Ren and D. Sun, *Objective Bayesian analysis for CAR models*, *Ann Inst Stat Math*, vol. 65, no. 3, pp. 457–472, Jun. 2013.
26. D. Lee, *CARBAYES: An R Package for Bayesian Spatial Modeling with Conditional Autoregressive Priors*, *J. Stat. Soft.*, vol. 55, no. 13, 2013.
27. E. W. Duncan, N. M. White, and K. Mengersen *Spatial smoothing in Bayesian models: a comparison of weights matrix specifications and their impact on inference*, *International Journal of Health Geographics*, vol. 16, no. 1, pp. 47, 2017.
28. R. A. Zarate *Conditional autoregressive models : implications for inference*, The University of Texas at Austin v2024.
29. E. Aldrian and Y. S. Djamil, *Spatio-temporal climatic change of rainfall in East Java Indonesia*, *International Journal of Climatology*, vol. 28, no. 4, pp. 435-448, 2008.



30. M. D. Purnama and M. E. Mustafidah *Relationship Between Temperature and Humidity on Rainfall: A Multiple Linear Regression Analysis*, Engineering, Mathematics and Computer Science Journal (EMACS), vol. 6, no.2, pp. 151-156. 2024.